Title: Lateralized phenotypic differences in females in the intrahippocampal kainic acid mouse model of temporal lobe epilepsy

Abbreviated title: Lateralized phenotypes in female mice with epilepsy

Authors: Cathryn A. Cutia*[1], Leanna K. Leverton*[2], Xiyu Ge[2], Rana Youssef[2], Lori T. Raetzman[1,2], and Catherine A. Christian-Hinman[1,2,3]

(*Equal contribution)

Affiliations: [1]Neuroscience Program; [2]Department of Molecular and Integrative Physiology; [3]Beckman Institute for Advanced Science and Technology, University of Illinois Urbana-Champaign, Urbana, IL, 61801 USA

Author contributions: C.A.C.-H. designed research; C.A.C., L.K.L., X.G., and R.Y. performed research; C.A.C., L.K.L., X.G, L.T.R., and C.A.C.-H. analyzed data; C.A.C. and C.A.C.-H. wrote the paper.

Corresponding author:

Catherine A. Christian-Hinman, Ph.D.

407 S. Goodwin Ave.

Urbana, IL 61801 USA

Phone: (217) 244-8230

Email: cathchri@illinois.edu

Number of Figures: 8

Number of Tables: 7

Number of Multimedia: 0

Number of words for Abstract: 249

Number of words for Significance: 120

Number of words for Introduction: 744

Number of words for Discussion: 2083

Acknowledgements:

We thank Karen Doty for performing ovary sectioning and staining, Jiang Li for assistance with pilot studies for this project, and Lola Lozano and Laxmi Manisha Naganatanahalli for assistance with estrous cycle monitoring and preparing tissue for histology.

Conflict of interest:

Authors report no conflict of interest.

Funding sources:

This work was supported by the National Institutes of Health (NIH)/National Institute of Neurological Disorders and Stroke and the NIH Office of Research on Women's Health through grants R03 NS103029 and R01 NS105825 (C.A.C.-H.).

Abstract

Clinical evidence indicates that patients with temporal lobe epilepsy (TLE) often show differential outcomes of comorbid conditions dependent on the lateralization of the seizure focus. However, whether a left or right seizure focus produces differential effects on comorbid outcomes has not been investigated in a rodent model of chronic recurrent seizures. Here, we used the intrahippocampal kainic acid (IHKA) mouse model of TLE to determine whether targeting of left or right dorsal hippocampus for injection produces different outcomes in hippocampal sclerosis, body weight gain, and multiple measures of reproductive endocrine dysfunction in female mice. At one, two, and four months after injection, *in vivo* measurements of estrous cycles and weight were followed by *ex vivo* examination of hippocampal sclerosis, circulating ovarian hormone and corticosterone levels, ovarian morphology, and pituitary gene expression. IHKA mice with right-targeted injection (IHKA-R) showed greater granule cell dispersion and pituitary *Fshb* expression compared to mice with left-targeted injection (IHKA-L). By contrast, pituitary expression of *Lhb* and *Gnrhr* were higher in IHKA-L mice compared to IHKA-R, but these values were not different from respective saline-injected controls. IHKA-L mice also showed an increased rate of weight gain compared to IHKA-R mice. Disruptions to estrous cyclicity, however, were similar in both IHKA-L and IHKA-R mice. These findings indicate that although major reproductive endocrine dysfunction phenotypes present similarly after targeting left or right dorsal hippocampus in the IHKA model of TLE, distinct latent mechanisms based on lateralization of seizure focus may contribute to produce similar emergent reproductive endocrine outcomes.

Significance Statement

People with epilepsy often develop comorbidities dependent on the side of the brain in which the seizures originate. However, the mechanisms linking laterality of seizure initiation side to different comorbidities are unknown. Here, we examined whether injection of kainic acid in the left or right hippocampus, a model of temporal lobe epilepsy, produces differential effects on hippocampal damage, weight gain, and measurements of female reproductive endocrine function in female mice. We found that hippocampal sclerosis, pituitary gene expression, and weight gain are influenced by the side of injection. These results are the first demonstration of changes in pituitary gene expression in a model of epilepsy and indicate that the hemisphere targeted in the intrahippocampal kainic acid model impacts phenotypic outcomes.

Introduction

Temporal lobe epilepsy (TLE) is the most prevalent form of focal epilepsy in adults (Engel, 2001). Patients with TLE commonly develop comorbid conditions such as cognitive impairment (Helmstaedter & Kockelmann, 2006), psychopathologies (Kandratavicius et al., 2012), and reproductive endocrine dysfunction (Herzog et al., 1986b, 1986a). Such comorbidities likely occur as results of a number of structural and functional abnormalities that develop both within the temporal lobe (Berkovic et al., 1991; Blümcke et al., 2002; Sutula et al., 1989) and elsewhere in the brain (Gross et al., 2006; Keller & Roberts, 2008; Campos et al., 2016). As the human brain shows a high level of structural and functional lateralization (Gazzaniga, 1995), such abnormalities can manifest differently based on the hemisphere in which the seizure focus, the site of seizure origination, resides. For example, patients with left-sided seizure foci often display more widespread abnormalities affecting the contralateral hemisphere than patients with right-sided seizure foci (Campos et al., 2016; Coan et al., 2009; Haneef et al., 2014; Keller et al., 2012). Furthermore, there is some evidence to suggest that cognitive impairment shows lateralization based on seizure focus as patients with left-sided seizure foci exhibit more cognitive impairment than those with a right-sided focus (Alessio et al., 2006; Bonilha et al., 2007; Phuong et al., 2021).

Prominent evidence for differential comorbid outcomes based on seizure focus lateralization lies in the clinical findings of reproductive endocrine dysfunction among women with TLE. Specifically, women with left temporal lobe seizure foci have increased rates of developing polycystic ovary syndrome (PCOS), whereas those with right-sided foci exhibit higher rates of hypothalamic amenorrhea and hypogonadotropic hypogonadism (Herzog, 1993; Herzog et al., 1986b; Kalinin & Zheleznova, 2007). Therefore, it appears that the laterality of the epileptic focus could be a significant risk factor for particular reproductive endocrine disorders or other outcomes, but the mechanisms producing this relationship remain unknown. Furthermore,

this correlation has been difficult to replicate in animal models of TLE; one study in rats found no difference in impacts on the estrous cycle after kindling the left or right amygdala (Hum et al., 2009). To date, no animal model of chronic epilepsy with recurrent spontaneous seizures has definitively shown differential effects of seizure focus lateralization on endocrine function or other phenotypic outcomes. Characterization of animal models investigating the impacts of left- vs. right-sided seizure foci could enable the study of mechanisms linking lateralization of epileptic focus to comorbid reproductive endocrine disorders and other distinct structural or functional changes. Furthermore, such an investigation would indicate whether lateralization of the epileptogenic insult in animal models of TLE contributes to differential experimental outcomes.

Several rodent models of epilepsy exhibit reproductive endocrine dysfunction in the form of disrupted estrous cycles in females (Amado et al., 1993; Christian et al., 2020; Edwards et al., 1999; Scharfman et al., 2008) and thus could potentially be used to study distinct outcomes of differentially targeted injection sites. Of these models, the intrahippocampal kainic acid (IHKA) mouse model not only leads to disruption in cycles (Li et al., 2017), but also shows similar histological and seizure patterning characteristics as human TLE (Bouilleret et al., 1999; Gröticke et al., 2008; Riban et al., 2002). This model also allows for the epileptogenic insult to be discretely targeted to the left or right hemisphere to develop a specific, lateralized seizure focus similar to those often seen in patients with TLE.

The pituitary gonadotropins, luteinizing hormone (LH) and follicle-stimulating hormone (FSH), are largely responsible for gonadal steroidogenesis and ovarian follicle development necessary for normal reproduction. The expression of gonadotropins at the pituitary is initiated when gonadotropin-releasing hormone (GnRH) binds its receptor, GnRH-R, at the pituitary. *Gnrhr* transcription is enhanced by increased amounts of GnRH (Cheon et al., 1999), or by elevations in circulating estradiol levels preceding the preovulatory LH surge (Yasin et al., 1995). Therefore, understanding expression levels of the functional subunits of these hormones

at the pituitary level is vital to understand input to the system and gives basic insight into the functional output. However, changes in pituitary gene expression have not been studied in an animal model of epilepsy.

Here, the phenotypic effects of left- versus right-sided dorsal hippocampal KA injection were comprehensively compared in adult female mice to test the hypothesis that differential outcomes are produced based on the side targeted for injection. Hippocampal sclerosis, pituitary gonadotropin gene expression levels, estrous cycle lengths, ovarian histology, gonadal and stress hormone levels, and post-injection weight gain were assessed across several time points after injection.

Materials and Methods

Animals and estrous cycle monitoring

All animal procedures complied with the ARRIVE guidelines and were approved by the Institutional Animal Care and Use Committee of the University of Illinois Urbana-Champaign. Female C57BL/6J mice (#000664, Jackson Laboratories) were purchased for delivery at 6 weeks of age and housed in a 14:10 h light:dark cycle with food and water available *ad libitum*. Starting 5 days after arrival, daily estrous cycle monitoring was performed between 0900 to 1100 h (relative to 1900 h lights off time) using a vaginal cytology protocol described previously (Pantier et al., 2019). Mice were assessed for a minimum of 14 days to verify regular cycling prior to saline/KA injection as described below. As outlined in **Figure 1**, the mice followed a timeline of estrous cycling that resumed beginning 3 weeks after injection for a minimum of 14 days, after which a subset of mice were euthanized by decapitation for tissue collection (1-month groups). At 7 weeks post-injection, the remaining mice resumed cycle monitoring for a minimum of 14 days, and a second subset was collected (2-months groups). At 15 weeks post-injection, the remaining mice resumed cycle monitoring again, and samples were collected for

the four-month groups. Cycle length (period) was calculated as the number of days required to progress from one day of estrus through each stage to the next day of estrus. Cycle lengths of 7 days or more were categorized as long cycles (Li et al., 2018).

IHKA injection surgeries and post-operative acute seizure video monitoring

Mice aged postnatal day 56 and older underwent stereotaxic unilateral injection of KA (Tocris Bioscience; 50 nL of 20 mM prepared in 0.9% sterile saline) into the left or right dorsal hippocampal region (from Bregma: 2.0 mm posterior, 1.5 mm lateral, 1.4 mm ventral to the cortical surface) as previously described (Li et al., 2017). All injections were performed on diestrus. Controls were injected with the same volume of saline at the same location. All surgeries were performed under isoflurane anesthesia (2-3%, vaporized in 100% oxygen). During recovery immediately after injection, IHKA mice were video recorded (iSpyConnect) following injection via webcam (Logitech C930e). Videos were scored using the Racine scale (Racine, 1972), and the time and stage of the first behavioral seizure at or above stage 3 were recorded.

Tissue collection

All tissue collections were performed on diestrus between 1200 and 1600 h. Mouse weights were recorded prior to euthanasia. Mice were euthanized via decapitation. The trunk blood, brain, pituitary gland, and ovaries were collected. Trunk blood was stored at 4°C for 24 h, then spun in a centrifuge for 10-15 minutes at 4°C. Serum was then pipetted off and stored at -80°C. Brains were bulk-fixed at 4°C in 4% paraformaldehyde (Sigma-Aldrich 158127) for 24 h, then switched to 30% sucrose with 5% sodium azide (ACROS Organics 19038-1000) and stored at 4°C. Pituitaries were stored in RNAlater Stabilization Solution (Invitrogen, AM7020) at -20°C.

Ovaries were stored in 10% formalin at 4°C overnight, then switched to 100% ethanol and stored at 4°C.

Hippocampal sclerosis quantification

40-μm coronal hippocampal sections were collected using a freezing microtome (SM 2010R, Leica Biosystems). Four to six sections per mouse from the dorsal hippocampal region were used for evaluation of hippocampal sclerosis by cresyl violet (Nissl) staining and/or gliosis by glial fibrillary acidic protein (GFAP) staining. For cresyl violet staining, sections were mounted on charged glass slides, stained with cresyl violet (Sigma-Aldrich C5042) for 12 minutes at room temperature (~22°C), dehydrated with graded ethanol solutions (70-100%), cleaned in xylene, and coverslipped with Permount. For GFAP immunofluorescence, sections were incubated with an anti-GFAP mouse monoclonal antibody (1:1000, Sigma-Aldrich G3893) for 48 h at 4°C on a shaker, followed by incubation with DyLight 594 horse anti-mouse secondary (1:1000, Vector DI-2594) for 2 h at room temperature on a shaker. Sections were then mounted on charged glass slides and coverslipped using Vectashield Hardset Antifade Mounting Medium with DAPI (Vector Laboratories H-1500). Image acquisition was performed using an Olympus BX43 brightfield and fluorescence microscope equipped with a Q-Color 3 camera and QCapture 6 software (QImaging). The degree of hippocampal damage produced after IHKA injection was quantified by measuring the surface area of the dentate gyrus granule cell layer and hilar regions in ImageJ. To account for normal variations in granule cell layer area in different regions of the hippocampus, the relative distance from Bregma was attained by comparisons to a mouse brain atlas (Paxinos & Franklin, 2019) for each hippocampal section. Ipsilateral and contralateral hippocampal regions with the same distance from Bregma were compared to one another to determine the ipsilateral:contralateral ratio.

Hormone assays

Enzyme-linked immunosorbent assays (ELISAs) for progesterone, estradiol, testosterone, and corticosterone were performed on trunk blood serum samples according to the manufacturers' instructions (progesterone: IBL America (IB79183); estradiol: Calbiotech (ES180S-100); testosterone: IBL America (IB79174); corticosterone: Arbor Assays (K014-H1)). As needed, samples were diluted to match the volume required for the testing. Samples were run in duplicate where appropriate and the average of the duplicate was used as the final hormone concentration value for each mouse. Intra-assay coefficient of variation (CV) values were calculated from the standard deviations within plates. Samples with CV values higher than 10 were excluded from the dataset, and plate variation was controlled for as a factor in statistical analyses.

Ovary histology and follicle counts

Both left and right ovaries were paraffin-embedded, and six consecutive sections of 5-μm thickness were collected from each ovary and stained with hematoxylin and eosin. An investigator blinded to treatment group screened the sections to quantify the number of primary, secondary, and antral follicles, and corpora lutea. Follicles were defined as primary, secondary, or antral according to characteristic morphology (Myers et al., 2004). The numbers of each type of ovarian follicle and corpora lutea were counted from both the left and right ovaries of each mouse and averaged to generate the final value for each mouse used in statistical analyses.

Pituitary qPCR

RNA was isolated from pituitaries using RNAqueous-Micro kits (Invitrogen). Total RNA was reverse-transcribed according to the manufacturer's instructions using the ProtoScript Strand

cDNA Synthesis kit (New England Biolabs) as previously described (Nantie et al., 2014). Oligonucleotide primers for *Lhb*, *Fshb* and *Gnrhr* (Life Technologies, **Table 1**) were used to amplify gene-specific transcripts by quantitative PCR (qPCR). The expression levels of genes of interest were normalized to peptidylprolyl isomerase A (*Ppia)* mRNA levels; *Ppia* is a common reference gene used as an internal control. The data were analyzed using the standard comparative cycle threshold value method ($2^{-\Delta\Delta Ct}$).

Statistics

Statistical analyses were conducted in R (R Core Team, 2021). Comparisons between control and IHKA treatment groups and left- vs. right-sided injection groups for hippocampal sclerosis, pituitary mRNA expression levels, and ovary follicle numbers were made using two-way ANOVAs followed by Tukey's *post hoc* tests. The data for hippocampal sclerosis and pituitary mRNA expression were log-transformed to achieve normality. Comparisons between treatment group and left or right injection for estrous cycle length were made using two-way ANOVAs and Tukey's *post hoc* tests for each time point. Comparisons between treatment group, left or right injection group, and time after injection (1, 2, or 4 months) for weight gain were made using three-way ANOVAs and Tukey's *post hoc* tests. As informed by Box-Cox normality plots, cycle length data were transformed with a negative exponent, and weight data were log-transformed to achieve normality. Comparisons between treatment group, left or right injection group, and ELISA plate group for hormone analyses were made using three-way ANOVAs. Hormone data were log-transformed to achieve normality. Normality was evaluated with Shapiro-Wilks tests. Correlations between degree of sclerosis and cycle length were made using Pearson's correlations, and comparisons of proportions of animals exhibiting sclerosis and long cycles were made with chi-square tests. The criterion for statistical significance was $p \leq 0.05$. Results are reported as means ± SEM.

Results

Evaluation of IHKA injection efficacy

To confirm the efficacy of IHKA injection, all IHKA mice (left-injected = IHKA-L; right-injected = IHKA-R) were screened for behavioral seizures directly following the injection (**Figure 2A**). Mice that did not show one or more seizures in the recording period underwent an evaluation for hippocampal sclerosis by Nissl staining, examined at either one, two, or four months after injection. Sections from mice that showed cell death in the CA1 region without significant granule cell layer dispersion underwent further confirmation through immunofluorescent GFAP staining to determine if gliosis was present. If neither sclerosis nor gliosis were present, and acute seizures were not confirmed in video screening, the mice were not included in final analyses, in accordance with criteria established previously (Li et al., 2018). A total of 4 of 12 IHKA-L and 2 of 12 IHKA-R mice with no recorded seizures did not meet these criteria to be included further in the study (**Figure 2B**). Overall, the success rate for meeting these criteria to enter IHKA mice in the study was ~90%.

IHKA-R animals have higher granular cell layer dispersion

To determine the impact of differentially targeting left or right dorsal IHKA injection on hippocampal sclerosis, an additional subset of IHKA animals that met the seizure screening and sclerosis/gliosis criterion (to total 86% of IHKA-L and 89% of IHKA-R mice included), as well as randomly selected saline-injected controls (Con-L and Con-R), was added to the histology dataset (**Figure 2C**). In the resulting analysis of ipsilateral:contralateral (I:C) ratio of the surface area of the dentate gyrus, there were higher levels of dispersion in IHKA mice than in controls ($F(1,85) = 13.81$, $p = 0.0004$, **Table 2**) in IHKA-L ($p = 0.005$) and IHKA-R groups ($p < 0.0001$) (**Figure 3A**). Moreover, side of injection yielded differences ($F(1,85) = 6.40$, $p = 0.01$, **Table 2**) as IHKA-R animals showed larger dispersion of the granule cell layer on average compared to

IHKA-L ($p = 0.04$), with no effect of time after injection ($F(2,77) = 1.82$, $p = 0.17$, **Figure 3B**). The proportion of mice that displayed prominent dispersion (defined as I:C > 1.5) was not different between IHKA-L and IHKA-R groups ($\chi^2 = 2.49$, $p = 0.11$, **Figure 3C**). Multiple thresholds of sclerosis ratios were tested for comparing proportions of mice in these two groups, but none produced a statistically significant difference in the proportions of dispersion. Overall, these data are the first demonstration of differential hippocampal damage based on the side of the epileptic focus in a mouse model of TLE.

Estrous cycles are longer in IHKA mice

Estrous cycle monitoring was performed at one, two, and four months after saline or IHKA injection, and the cycle length was subsequently derived for each time point (**Figure 4**). Cycle length was analyzed and reported as it is the most robust measure of disruption in IHKA mice (Li et al., 2017, 2018, 2020). There was no effect of time after injection on the mean cycle length ($F(2,419) = 1.15$, $p = 0.22$), but there were differential shifts in cyclicity across the months. At one month post-injection, longer cycles in comparison to respective control groups ($F(1, 209) = 9.23$, $p = 0.002$, **Table 3**) were observed in both IHKA-L ($p = 0.01$) and IHKA-R ($p = 0.003$), but this effect was not impacted by the side targeted for injection ($F(1, 209) = 0.14$, $p = 0.70$, **Figure 4B**). At two months post-injection, cycle length was still increased compared to controls ($F(1,148) =6.61$, $p = 0.01$, **Table 3**) in IHKA-L ($p = 0.05$) and IHKA-R ($p = 0.02$) mice, again with no effects of injection site ($F(1,148) = 0.49$, $p = 0.48$, **Figure 4B**). At four months post-injection, only IHKA-R mice still exhibited increased cycle length compared to controls ($p = 0.02$, **Figure 4B**), but the cycle length at this time was not different between IHKA-R and IHKA-L groups ($F(1,62) = 0.69$, $p = 0.41$, **Table 3**). The results were further analyzed to determine whether the proportion of mice developing lengthened cycles differed based on left or right injection, and the proportion of mice with long cycles was not found to be different from between IHKA-L and IHKA-R ($\chi^2 = 0.039$, $p = 0.84$, **Figure 4C**). There were significant differences,

however, in the proportion of IHKA-L mice that showed long cycles compared to Con-L at one month (χ^2 =5.15, p = 0.02, **Table 3**), and in IHKA-R compared to Con-R mice at one (χ^2 = 15.76, p = 7.2 x 10^{-5}) and four months χ^2 =6.68, p = 0.009). Overall, there were disruptions in cyclicity in all IHKA groups by one- and two-months post injection, but at four months only the IHKA-R animals showed significantly lengthened cycles in comparison to controls. These results confirm previous findings of estrous cycle disruption occurring by two months after injection in IHKA-R mice (Li et al., 2017, 2018, 2020) and demonstrate that disruption can also be seen at one and four months post-injection in this group. Furthermore, these results extend previous findings by indicating that IHKA-L mice follow similar trends as IHKA-R in cycle disruption for the first two months after injection.

The presence of IHKA mice with less granule cell dispersion (**Figure 3**), as well as the proportion of IHKA females that maintain a normal estrous cycle following injection (Li et al., 2017, 2018, 2020)(**Figure 4**), suggested that the degree of cycle disruption and the amount of sclerosis may be correlated. However, there was no correlation between degree of sclerosis and estrous cycle length (r^2 = 0.03, p = 0.13).

Ovarian hormones and corticosterone are unchanged after IHKA injection

Changes in ovarian hormones such as estradiol, progesterone, and testosterone could potentially contribute to disruptions in estrous cyclicity. In a previous study, a decrease in progesterone was observed at two months after injection in IHKA-R mice with long cycles, and IHKA-R mice with both long and regular cycles lacked the decrease in estradiol levels on estrus compared to diestrus seen in controls (Li et al., 2018). Furthermore, altered serum levels of these hormones have been reported in other rodent models of TLE that also display cycle disruption (Amado et al., 1993; Scharfman et al., 2008). Therefore, the trunk blood serum of IHKA-L, IHKA-R, Con-L, and Con-R mice collected on diestrus at one, two-, and four-months

post-injection was analyzed through ELISA for levels of estradiol, progesterone, and testosterone. The time after injection did not have an effect on the concentrations of estradiol ($F(2,96) = 0.56$, $p = 0.57$), progesterone ($F(2,105) = 0.56$, $p = 0.58$), or testosterone ($F(2,121) = 1.10$, $p = 0.33$) (**Figure 5**). In addition, IHKA groups did not show differences in concentrations of estradiol ($F(1,104) = 0.44$, $p = 0.50$, **Table 4**), progesterone ($F(1,113) = 1.95$, $p=0.17$), or testosterone ($F(1,129) = 0.02$, $p=0.88$) in comparison to controls. There were also no effects of injection side on the concentration of estradiol ($F(1,104) = 0.22$, $p=0.63$, **Table 4**), progesterone ($F(1,113) = 0.13$, $p=0.71$), or testosterone ($F(1,129) = 0.45$, $p =0.5$). Furthermore, there was no correlation between progesterone levels and cycle length ($r^2 = 0.007$, $p = 0.52$), in accordance with a previous study (Li et al., 2018).

High levels of the stress hormone corticosterone have been observed in animal models of epilepsy (Mazarati et al., 2009), potentially due to seizure-induced hyperexcitability of the hypothalamic-pituitary-adrenal axis (O'Toole et al., 2014). Increased corticosterone levels have also been known to drive increased seizure activity (Castro et al., 2012), and corticosterone can also disrupt the pulsatile pattern of pituitary LH release and subsequently alter the production of gonadal steroids (Kamel & Kubajak, 1987). Therefore, to evaluate the stress level of the animals between treatment groups and to ensure that stress of the treatment groups was not contributing to other hormonal findings, corticosterone was measured for the subset of animals for which sufficient serum remained after measuring the ovarian hormones. This evaluation showed that there was no significant effect of treatment ($F(1,64) = 1.55$, $p = 0.21$, **Table 4**) or injection side ($F(1,64) = 0.02$, $p = 0.87$) on basal corticosterone concentrations (IHKA-R: 1122.03 ± 603.22 pg/ml, $n = 23$; IHKA-L: 1124.16 ± 637.30 pg/ml, $n = 14$; Con-R: 985.15 ± 460.98 pg/ml, $n = 27$; Con-L: 1020.11 ± 960.31 pg/ml, $n = 5$).

Numbers of ovarian follicles and corpora lutea are not changed after IHKA injection

The duration of time after injection had no effects on the number of primary ($F(2,198) = 0.30$, $p = 0.74$), secondary ($F(2,198) = 2.90$, $p = 0.07$), or antral ($F(2,198) = 0.48$, $p = 0.62$) follicles or corpora lutea ($F(2,198) = 0.39$, $p = 0.68$) in the ovaries. Therefore, the groups were collapsed across time of collection for further analysis. No significant differences in follicle or corpora lutea counts based on side of injection or saline vs. IHKA treatment were present (**Table 5**). Furthermore, no ovaries displayed cysts. These findings support and extend previous work that found no ovarian cysts or differences in follicle or corpora lutea counts in IHKA-R mice (Li et al., 2017).

Differences between IHKA-L and IHKA-R mice in pituitary expression of gonadotropin and Gnrhr *genes*

To evaluate the contribution of the pituitary to potential disruptions in reproductive function, *Fshb*, *Lhb,* and *Gnrhr* mRNA expression were measured from the pituitaries of mice collected at two months after injection using qPCR. *Fshb* expression was impacted by injection side ($F(1,41) =6.87$, $p = 0.01$, **Table 6**), and type ($F(1,41) = 5.88$, $p = 0.02$) as levels were higher in IHKA-R than IHKA-L groups ($p = 0.048$), and in IHKA-R compared to Con-R ($p = 0.004$) (**Figure 6A**). *Lhb* expression was also impacted by injection side ($F(1,41) = 10.19$, $p = 0.003$, **Table 6**) as IHKA-L mice showed higher expression of *Lhb* than IHKA-R ($p = 0.01$), but neither IHKA groups were significantly different from corresponding controls ($F(1,41) = 4.35$, $p = 0.04$ left: $p = 0.17$; right: $p = 0.99$, **Figure 6B**). *Gnrhr* expression showed similar patterns as *Lhb,* with expression impacted by injection side ($F(1,52) = 5.61$, $p = 0.02$, **Table 6**) with higher expression in IHKA-L than IHKA-R mice ($p = 0.05$), but neither group differed from corresponding saline controls ($F(1,52) = 4.53$ $p = 0.04$; left: $p = 0.1577$; right: $p = 0.68$) **Figure 6C**). Overall, IHKA-R mice showed the highest elevation of *Fshb* expression, and IHKA-L showed higher *Lhb* and *Gnrhr* expression than IHKA-R mice.

IHKA-L mice gain weight at an increased rate

In a previous study, IHKA-R mice were observed to have increased weight gain compared to controls (Li et al., 2017). To evaluate potential differences in weight gain based on side of injection, body weights were measured at the times of injection surgery and euthanasia. In comparison to respective saline controls, IHKA-L animals had higher weight gain at one month after injection ($p = 0.0012$) and borderline significantly higher weight gain at two months post-injection ($p = 0.053$) (**Figure 7**). However, the average weight gain in IHKA-L mice was not different based on time after injection. By contrast, IHKA-R mice did not display weight gain that differed from Con-R mice at any time after injection (**Table 7**) but mice measured at four months after injection showed greater weight gain compared to those measured at one month ($p = 0.0001$). This result was similar to that observed in Con-L and -R, which also showed increased weight gain in mice measured at two months after injection compared to those measured at one month (Con-L: $p = 0.02$, Con-R: $p = 0.002$) as well as those mice measured at two months compared to those at four months (Con-L: $p = 0.008$, Con-R: $p = 0.009$). Overall, IHKA-L mice initially gained weight at a faster rate but then plateaued at a stable weight, whereas IHKA-R mice showed a more gradual weight gain similar to that observed in controls over the same age range.

Discussion

This study focused on female mice to investigate the effects of left vs. right-targeted injection as it is largely women rather than men with TLE that demonstrate evidence for differential reproductive endocrine outcomes based on laterality of the seizure focus (Herzog, 1993; Kalinin & Zheleznova, 2007). The findings in the present study indicate that targeting left or right dorsal hippocampus for KA injection has implications on the level of hippocampal

sclerosis, phenotypes of pituitary gene expression, and the degree of weight gain after injection in female C57BL/6J mice. However, there do not seem to be large phenotypic differences in reproductive endocrine dysfunction presentation. The lack of differences in estrous cycle disruption based on side of injection seen in this model of TLE, as well as a lack of impact on ovarian morphology, supports and extends previous findings obtained in IHKA-R mice only (Li et al., 2017). Overall, these findings suggest that distinct latent mechanisms based on lateralization of seizure focus may contribute to produce similar emergent outcomes.

Lateralized differences in hippocampal sclerosis in IHKA mice

The observed increase in granule cell layer dispersion and cell death in Ammon's horn is common to the IHKA model (Bielefeld et al., 2017; Rattka et al., 2013) and a similar histological phenotype is often observed in patients with TLE (Berkovic et al., 1991). The results from this study further serve to highlight that this model recapitulates the variety of histological morphologies seen in clinical TLE populations (Blümcke et al., 2013), as not all mice in the study with CA region cell death presented significant granule cell dispersion, and some IHKA mice did not exhibit sclerosis or gliosis.

The present work provides a novel finding of a greater amount of dispersion present in IHKA-R compared to IHKA-L mice. Although less lateralized than the human brain, mice show structural and functional asymmetries in the hippocampus; wild-type C57BL/6J mice show greater granule cell layer volume in the right hippocampal dentate gyrus compared to the left (Tabibnia et al., 1999), and optogenetic silencing of the left CA3 region can impair long term spatial memory, but silencing the right CA3 does not produce the same effect (Shipton et al., 2014). Of note, a number of molecular, microanatomical, and behavioral asymmetries that have been reported in the rodent hippocampus (Jordan, 2020) could contribute to such differential

presentation of this sclerosis. Intrinsic molecular asymmetries in mouse hippocampus, such as decreased expression of GluR1 in the cells of the left hippocampus compared to the right (Shinohara et al., 2008), could underlie differential responses to KA, resulting in the varied presentation of sclerosis in IHKA-L and -R animals. Higher severity of status epilepticus or chronic seizures that originate in the right temporal lobe versus the left could also contribute to differential death and reorganization of hippocampal cell populations. EEG recordings are needed to investigate the contributions of seizure severity to hippocampal neuron damage in IHKA-L and IHKA-R mice; such studies, beyond the scope of the present work, are currently ongoing in our lab.

Lateralized expression of gonadotropin and Gnrhr *genes in pituitaries of IHKA mice*

To understand whether changes at the level of the pituitary could at least partially underlie downstream reproductive endocrine disruption, mRNA expression levels of *Fshb*, *Lhb*, and *Gnrhr* were evaluated. The lack of differences in *Lhb* and *Gnrhr* levels in IHKA mice in comparison to controls, and only a mild increase in expression of each gene in IHKA-R compared to IHKA-L mice, suggest an inherent difference in the pituitary's response to the lateralization of damage inflicted by the injection, but that the presence of epilepsy had no effect on the transcription of these genes. By contrast, only IHKA-R mice showed increased expression of *Fshb*. *Fshb* synthesis is regulated not only by GnRH, but also by several other factors including inhibins, activins, and follistatins (Ying, 1988). *Lhb*, however, is mainly regulated by GnRH. As changes in inhibins, activins, and follistatins would only have effects on *Fshb*, these factors, rather than GnRH, may be more likely candidates in mediating this change. However, it should be noted that ovarian cytology was unchanged, and inhibins are produced from ovarian follicles and corpora lutea (Woodruff & Mayo, 1990). It is possible that locally produced activins (Corrigan et al., 1991) and follistatins (Ueno et al., 1987) differentially exert

effects within the pituitary based on the side of hippocampus targeted for KA injection. Further evidence supporting a postulated role for these locally produced factors is the association of *Fshb* transcription with lower GnRH pulse frequency (Bernard & Brûlé, 2020); if GnRH pulse frequency were decreased, one might expect a decrease in *Gnrhr* expression as well, but this was not the case. However, there may be altered release patterns of GnRH due to changes in the function of GnRH and other hypothalamic neurons (Li et al., 2018), and the pituitary perhaps responds to this change by compensatorily maintaining GnRH-R expression so that activation is not subsequently decreased. Importantly, the present findings are the first to demonstrate changes in pituitary gene expression in an animal model of epilepsy. Furthermore, differences in expression profiles based on the side of IHKA injection indicate asymmetries in the seizure focus can have implications at the level of the pituitary.

Lengthening of estrous cycles in IHKA mice is irrespective of injection site

The lengthening of the average estrous cycle period is a phenotype that has been previously characterized in IHKA-R mice (Li et al., 2017, 2018, 2020) as well as in other rodent models of TLE (Amado et al., 1993; Edwards et al., 1999; Scharfman et al., 2008). It has been previously noted that cycle disruption in IHKA-R mice did not develop until at least 6 weeks after injection (Li et al., 2017). In the present study, which incorporates a larger number of mice, estrous cycles were disrupted at one, two, and four months after injection. There may also be a more persistent effect in IHKA-R than in IHKA-L mice, potentially due to differential underlying mechanisms of the elongated cycles, as the degree of effect on cycle length diminished by four months in IHKA-L but not IHKA-R mice.

A lack of effect of the side of hippocampal injection on estrous cycle disruption was also seen in a previous study investigating the effects of left- vs. right-sided amygdala kindling in rats

(Hum et al., 2009). This finding is consistent with the present results in IHKA mice, in which estrous cycle disruption was prominent but the side targeted for injection largely did not affect the overall outcome of the disruption. More prolonged estrous cycle disruption observed in IHKA-R than in IHKA-L mice might be linked to the asymmetries seen in the hippocampal structures, and the pituitary gene expression in these animals. However, estrous cycle disruption was otherwise largely phenotypically similar in both IHKA groups. Therefore, it could be that similar emergent reproductive endocrine phenotypes are produced from distinct underlying mechanisms at the neural and pituitary levels, thus masking the ability of IHKA or other mouse models to recapitulate the distinct reproductive endocrine outcomes seen in TLE patients with lateralized seizure foci.

Rate of post-injection weight gain in IHKA mice differs based on side targeted for injection

Incremental weight gain over time has been reported within the C57BL/6J mouse strain from Jackson Laboratories (Fahlström et al., 2011), which aligns with the patterns observed here in both saline-injected groups. The faster rate of weight gain in IHKA-L compared to Con-L mice is consistent with clinical findings of a potential correlation between left hippocampal atrophy and obesity in children (Mestre et al., 2017). It is also consistent with data from male rats indicating that orexigenic activation of the melanocortin system dominates on the left hypothalamic side (Kiss et al., 2020). In addition, female patients with TLE with left seizure foci have a greater risk of developing PCOS (Herzog et al., 1986b), and women with PCOS typically have higher weight gain than the general population (Teede et al., 2013). The present findings suggest that the left hippocampus, and efferents to left hypothalamic regions, may have greater implications in weight regulation than the right hippocampus. It should be noted that the lack of difference in weight gain of IHKA-R mice in this study contrasts with previous findings of elevated body weight in IHKA-R female mice compared with controls (Li et al., 2017). Although

the reported weight gain in the previous study for IHKA-R animals was higher than that observed in the present cohort of IHKA-R mice, it was similar to that of the IHKA-L animals in this study. A difference between the number of animals examined in each study, with a smaller cohort examined previously, as well as environmental factors including intermittent construction noise and vibration during the time of the present work, could have contributed to these discrepant results.

Ovarian hormones, follicles, and corpora lutea are unaffected by IHKA injection, or side of hippocampus targeted for injection

The lack of changes in the number of corpora lutea or follicles due to any of the treatment factors aligns with previous evaluations of ovarian morphology in IHKA-R mice (Li et al., 2017). In IHKA mice, no cysts were present in the ovary samples, and no changes in testosterone levels were observed. By contrast, systemic pilocarpine-treated female rats with epilepsy have shown prominent development of cysts and elevated testosterone (Scharfman et al., 2008); it remains unclear whether this difference represents a distinction based on chemoconvulsant mechanism of action and/or mode of injection, or a species difference between mice and rats. In this regard, C57BL/6 mice may be more resistant to age-related cyst development in comparison to other mouse strains (Kon et al., 2007), and mouse models of PCOS typically require powerful endocrine manipulations including prenatal androgenization (Sullivan & Moenter, 2004) or chronic treatment with the aromatase inhibitor letrozole (Kauffman et al., 2015) to drive the presentation of cysts.

It should be noted that previous findings suggested that IHKA mice with long cycles had altered progesterone levels correlated to cycle length (Li et al., 2018). This discrepancy could be attributed to tissue collections being performed at slightly different times of day in each study, or

to strain differences between the two studies (although the transgenic mice used in the previous study were on the C57BL/6J background). The previous study also used a population of mice bred in-house, whereas the mice in the present study were purchased and shipped to our facility at 6 weeks of age. Another factor could be that the ELISAs to measure hormone levels in the previous and present studies were performed in separate labs using different equipment. It should be noted, however, that similar ranges of progesterone levels were measured in both studies, suggesting that methodology is unlikely to be the prevailing source of variance. Corticosterone has been known to disrupt the pulsatile release of LH and is linked with altered steroidogenesis at the ovary (Kamel & Kubajak, 1987). As corticosterone levels were unchanged in this study, however, there were no indications that physiological stress on the animals within the studies played a factor in the gonadal hormone results.

Concluding remarks

The present findings provide novel evidence of lateralized differences in phenotypic outcomes in the IHKA mouse model of TLE, with significant differences in hippocampal sclerosis presentation, pituitary gonadotropin gene expression, and weight gain between IHKA-L and -R animals (**Figure 8**). The lateralized differences in hippocampal sclerosis and pituitary gonadotropin gene expression, together with a lack of difference in estrous cycle disruption phenotype based on injection site, indicate that there may be differential “latent” mechanisms that produce similar comorbid reproductive endocrine outcomes. This concept is akin to the recent postulate of latent sex differences in hippocampal function, in which the emergent output in males and females is similar but the underlying mechanisms are distinct (Jain et al., 2019; Koss et al., 2018). Whether this effect reflects compensation at the level of the pituitary, or effects further downstream in the hypothalamic-pituitary-ovarian axis, remains to be determined.

Further analysis of pituitary gonadotropin release is needed to confirm if there is a change in the amount of functional FSH or LH levels that could promote cycle disruption in IHKA mice.

In summary, the present work demonstrates distinct lateralized differences in phenotypic outcome based on the side of the hippocampus targeted for injection in the IHKA model, spanning from the level of the hippocampus to the pituitary to whole body weight. This work thus demonstrates the importance of choosing the appropriate hemisphere of hippocampus for initial epileptogenic insult and provides a foundation for future experimental design.

References:

Alessio, A., Bonilha, L., Rorden, C., Kobayashi, E., Min, L. L., Damasceno, B. P., & Cendes, F. (2006). Memory and language impairments and their relationships to hippocampal and perirhinal cortex damage in patients with medial temporal lobe epilepsy. *Epilepsy & Behavior*, *8*(3), 593–600. https://doi.org/10.1016/j.yebeh.2006.01.007

Amado, D., Cavalheiro, E. A., & Bentivoglio, M. (1993). Epilepsy and hormonal regulation: The patterns of GnRH and galanin immunoreactivity in the hypothalamus of epileptic female rats. *Epilepsy Research*, *14*(2), 149–159. https://doi.org/10.1016/0920-1211(93)90019-4

Berkovic, S. F., Andermann, F., Olivier, A., Ethier, R., Melanson, D., Robitaille, Y., Kuzniecky, R., Peters, T., & Feindel, W. (1991). Hippocampal sclerosis in temporal lobe epilepsy demonstrated by magnetic resonance imaging. *Annals of Neurology*, *29*(2), 175–182. https://doi.org/10.1002/ana.410290210

Bernard, D. J., & Brûlé, E. (2020). Chapter 7 - Anterior Pituitary: Glycoprotein Hormones From Gonadotrope (FSH and LH) and Thyrotrope (TSH) Cells. In G. Litwack (Ed.), *Hormonal Signaling in Biology and Medicine* (pp. 119–144). Academic Press. https://doi.org/10.1016/B978-0-12-813814-4.00007-9

Bielefeld, P., Sierra, A., Encinas, J. M., Maletic-Savatic, M., Anderson, A., & Fitzsimons, C. P. (2017). A Standardized Protocol for Stereotaxic Intrahippocampal Administration of Kainic Acid Combined with Electroencephalographic Seizure Monitoring in Mice. *Frontiers in Neuroscience*, *11*, 160. https://doi.org/10.3389/fnins.2017.00160

Blümcke, I., Thom, M., Aronica, E., Armstrong, D. D., Bartolomei, F., Bernasconi, A., Bernasconi, N., Bien, C. G., Cendes, F., Coras, R., Cross, J. H., Jacques, T. S., Kahane, P., Mathern, G. W., Miyata, H., Moshé, S. L., Oz, B., Özkara, Ç., Perucca, E., … Spreafico, R. (2013). International consensus classification of hippocampal sclerosis in temporal lobe epilepsy: A Task Force report from the ILAE Commission on Diagnostic Methods. *Epilepsia*, *54*(7), 1315–1329. https://doi.org/10.1111/epi.12220

Blümcke, I., Thom, M., & Wiestler, O. D. (2002). Ammon's horn sclerosis: A maldevelopmental disorder associated with temporal lobe epilepsy. *Brain Pathology (Zurich, Switzerland)*, *12*(2), 199–211.

Bonilha, L., Rorden, C., Halford, J. J., Eckert, M., Appenzeller, S., Cendes, F., & Li, L. M. (2007). Asymmetrical extra-hippocampal grey matter loss related to hippocampal atrophy in patients with medial temporal lobe epilepsy. *Journal of Neurology, Neurosurgery & Psychiatry*, *78*(3), 286–294. https://doi.org/10.1136/jnnp.2006.103994

Bouilleret, V., Ridoux, V., Depaulis, A., Marescaux, C., Nehlig, A., & Le Gal La Salle, G. (1999). Recurrent seizures and hippocampal sclerosis following intrahippocampal kainate injection in adult mice: Electroencephalography, histopathology and synaptic reorganization similar to mesial temporal lobe epilepsy. *Neuroscience*, *89*(3), 717–729. https://doi.org/10.1016/s0306-4522(98)00401-1

Campos, B. M. de, Coan, A. C., Yasuda, C. L., Casseb, R. F., & Cendes, F. (2016). Large-scale brain networks are distinctly affected in right and left mesial temporal lobe epilepsy. *Human Brain Mapping*, *37*(9), 3137–3152. https://doi.org/10.1002/hbm.23231

Castro, O. W., Santos, V. R., Pun, R. Y. K., McKlveen, J. M., Batie, M., Holland, K. D., Gardner, M., Garcia-Cairasco, N., Herman, J. P., & Danzer, S. C. (2012). Impact of corticosterone treatment on spontaneous seizure frequency and epileptiform activity in mice with chronic epilepsy. *PloS One*, *7*(9), e46044. https://doi.org/10.1371/journal.pone.0046044

Cheon, M., Park, D., Kim, K., Park, S. D., & Ryu, K. (1999). Homologous upregulation of GnRH receptor mRNA by continuous GnRH in cultured rat pituitary cells. *Endocrine*, *11*(1), 49–55. https://doi.org/10.1385/ENDO:11:1:49

Christian, C. A., Reddy, D. S., Maguire, J., & Forcelli, P. A. (2020). Sex Differences in the Epilepsies and Associated Comorbidities: Implications for Use and Development of Pharmacotherapies. *Pharmacological Reviews*, *72*(4), 767–800. https://doi.org/10.1124/pr.119.017392

Coan, A. C., Appenzeller, S., Bonilha, L., Li, L. M., & Cendes, F. (2009). Seizure frequency and lateralization affect progression of atrophy in temporal lobe epilepsy. *Neurology*, *73*(11), 834–842. https://doi.org/10.1212/WNL.0b013e3181b783dd

Corrigan, A. Z., Bilezikjian, L. M., Carroll, R. S., Bald, L. N., Schmelzer, C. H., Fendly, B. M., Mason, A. J., Chin, W. W., Schwall, R. H., & Vale, W. (1991). Evidence for an autocrine role of activin B within rat anterior pituitary cultures. *Endocrinology*, *128*(3), 1682–1684. https://doi.org/10.1210/endo-128-3-1682

Edwards, H. E., Burnham, W. M., Ng, M. M., Asa, S., & MacLusky, N. J. (1999). Limbic seizures alter reproductive function in the female rat. *Epilepsia*, *40*(10), 1370–1377. https://doi.org/10.1111/j.1528-1157.1999.tb02007.x

Engel, J. (2001). Mesial temporal lobe epilepsy: What have we learned? *The Neuroscientist: A Review Journal Bringing Neurobiology, Neurology and Psychiatry*, *7*(4), 340–352. https://doi.org/10.1177/107385840100700410

Fahlström, A., Yu, Q., & Ulfhake, B. (2011). Behavioral changes in aging female C57BL/6 mice. *Neurobiology of Aging*, *32*(10), 1868–1880. https://doi.org/10.1016/j.neurobiolaging.2009.11.003

Gazzaniga, M. S. (1995). Principles of human brain organization derived from split-brain studies. *Neuron*, *14*(2), 217–228. https://doi.org/10.1016/0896-6273(95)90280-5

Gross, D. W., Concha, L., & Beaulieu, C. (2006). Extratemporal White Matter Abnormalities in Mesial Temporal Lobe Epilepsy Demonstrated with Diffusion Tensor Imaging. *Epilepsia*, *47*(8), 1360–1363. https://doi.org/10.1111/j.1528-1167.2006.00603.x

Gröticke, I., Hoffmann, K., & Löscher, W. (2008). Behavioral alterations in a mouse model of temporal lobe epilepsy induced by intrahippocampal injection of kainate. *Experimental Neurology*, *213*(1), 71–83. https://doi.org/10.1016/j.expneurol.2008.04.036

Haneef, Z., Lenartowicz, A., Yeh, H. J., Levin, H. S., Engel, J., & Stern, J. M. (2014). Functional connectivity of hippocampal networks in temporal lobe epilepsy. *Epilepsia*, *55*(1), 137–145. https://doi.org/10.1111/epi.12476

Helmstaedter, C., & Kockelmann, E. (2006). Cognitive Outcomes in Patients with Chronic Temporal Lobe Epilepsy. *Epilepsia*, *47*(s2), 96–98. https://doi.org/10.1111/j.1528-1167.2006.00702.x

Herzog, A. G. (1993). A relationship between particular reproductive endocrine disorders and the laterality of epileptiform discharges in women with epilepsy. *Neurology*, *43*(10), 1907–1910. https://doi.org/10.1212/wnl.43.10.1907

Herzog, A. G., Seibel, M. M., Schomer, D. L., Vaitukaitis, J. L., & Geschwind, N. (1986a). Reproductive endocrine disorders in men with partial seizures of temporal lobe origin. *Archives of Neurology*, *43*(4), 347–350. https://doi.org/10.1001/archneur.1986.00520040035015

Herzog, A. G., Seibel, M. M., Schomer, D. L., Vaitukaitis, J. L., & Geschwind, N. (1986b). Reproductive endocrine disorders in women with partial seizures of temporal lobe origin. *Archives of Neurology*, *43*(4), 341–346. https://doi.org/10.1001/archneur.1986.00520040029014

Hum, K. M., Megna, S., & Burnham, W. M. (2009). The effects of right and left amygdala kindling on the female reproductive system in rats. *Epilepsia*, *50*(4), 880–886. https://doi.org/10.1111/j.1528-1167.2008.01982.x

Jain, A., Huang, G. Z., & Woolley, C. S. (2019). Latent Sex Differences in Molecular Signaling That Underlies Excitatory Synaptic Potentiation in the Hippocampus. *The Journal of Neuroscience: The Official Journal of the Society for Neuroscience*, *39*(9), 1552–1565. https://doi.org/10.1523/JNEUROSCI.1897-18.2018

Jordan, J. T. (2020). The rodent hippocampus as a bilateral structure: A review of hemispheric lateralization. *Hippocampus*, *30*(3), 278–292. https://doi.org/10.1002/hipo.23188

Kalinin, V. V., & Zheleznova, E. V. (2007). Chronology and evolution of temporal lobe epilepsy and endocrine reproductive dysfunction in women: Relationships to side of focus and catameniality. *Epilepsy & Behavior: E&B*, *11*(2), 185–191. https://doi.org/10.1016/j.yebeh.2007.04.014

Kamel, F., & Kubajak, C. L. (1987). Modulation of gonadotropin secretion by corticosterone: Interaction with gonadal steroids and mechanism of action. *Endocrinology*, *121*(2), 561–568. https://doi.org/10.1210/endo-121-2-561

Kandratavicius, L., Lopes-Aguiar, C., Bueno-Júnior, L. S., Romcy-Pereira, R. N., Hallak, J. E. C., & Leite, J. P. (2012). Psychiatric comorbidities in temporal lobe epilepsy: Possible relationships between psychotic disorders and involvement of limbic circuits. *Revista Brasileira De Psiquiatria (Sao Paulo, Brazil: 1999)*, *34*(4), 454–466. https://doi.org/10.1016/j.rbp.2012.04.007

Kauffman, A. S., Thackray, V. G., Ryan, G. E., Tolson, K. P., Glidewell-Kenney, C. A., Semaan, S. J., Poling, M. C., Iwata, N., Breen, K. M., Duleba, A. J., Stener-Victorin, E., Shimasaki, S., Webster, N. J., & Mellon, P. L. (2015). A Novel Letrozole Model Recapitulates Both the Reproductive and Metabolic Phenotypes of Polycystic Ovary Syndrome in Female Mice. *Biology of Reproduction*, *93*(3), 69. https://doi.org/10.1095/biolreprod.115.131631

Keller, S. S., & Roberts, N. (2008). Voxel-based morphometry of temporal lobe epilepsy: An introduction and review of the literature. *Epilepsia*, *49*(5), 741–757. https://doi.org/10.1111/j.1528-1167.2007.01485.x

Keller, S. S., Schoene-Bake, J.-C., Gerdes, J. S., Weber, B., & Deppe, M. (2012). Concomitant Fractional Anisotropy and Volumetric Abnormalities in Temporal Lobe Epilepsy: Cross-Sectional Evidence for Progressive Neurologic Injury. *PLOS ONE*, *7*(10), e46791. https://doi.org/10.1371/journal.pone.0046791

Kiss, D. S., Toth, I., Jocsak, G., Bartha, T., Frenyo, L. V., Barany, Z., Horvath, T. L., & Zsarnovszky, A. (2020). Metabolic Lateralization in the Hypothalamus of Male Rats Related to Reproductive and Satiety States. *Reproductive Sciences (Thousand Oaks, Calif.)*, *27*(5), 1197–1205. https://doi.org/10.1007/s43032-019-00131-3

Kon, Y., Konno, A., Hashimoto, Y., & Endoh, D. (2007). Ovarian cysts in MRL/MpJ mice originate from rete ovarii. *Anatomia, Histologia, Embryologia*, *36*(3), 172–178. https://doi.org/10.1111/j.1439-0264.2006.00728.x

Koss, W. A., Haertel, J. M., Philippi, S. M., & Frick, K. M. (2018). Sex Differences in the Rapid Cell Signaling Mechanisms Underlying the Memory-Enhancing Effects of 17β-Estradiol. *ENeuro*, *5*(5), ENEURO.0267-18.2018. https://doi.org/10.1523/ENEURO.0267-18.2018

Li, J., Kim, J. S., Abejuela, V. A., Lamano, J. B., Klein, N. J., & Christian, C. A. (2017). Disrupted female estrous cyclicity in the intrahippocampal kainic acid mouse model of temporal lobe epilepsy. *Epilepsia Open*, *2*(1), 39–47. https://doi.org/10.1002/epi4.12026

Li, J., Leverton, L. K., Naganatanahalli, L. M., & Christian-Hinman, C. A. (2020). Seizure burden fluctuates with the female reproductive cycle in a mouse model of chronic temporal lobe epilepsy. *Experimental Neurology*, *334*, 113492. https://doi.org/10.1016/j.expneurol.2020.113492

Li, J., Robare, J. A., Gao, L., Ghane, M. A., Flaws, J. A., Nelson, M. E., & Christian, C. A. (2018). Dynamic and Sex-Specific Changes in Gonadotropin-Releasing Hormone Neuron Activity and Excitability in a Mouse Model of Temporal Lobe Epilepsy. *ENeuro*, *5*(5), ENEURO.0273-18.2018. https://doi.org/10.1523/ENEURO.0273-18.2018

Mazarati, A. M., Shin, D., Kwon, Y. S., Bragin, A., Pineda, E., Tio, D., Taylor, A. N., & Sankar, R. (2009). Elevated plasma corticosterone level and depressive behavior in experimental temporal lobe epilepsy. *Neurobiology of Disease*, *34*(3), 457–461. https://doi.org/10.1016/j.nbd.2009.02.018

Mestre, Z. L., Bischoff-Grethe, A., Eichen, D. M., Wierenga, C. E., Strong, D., & Boutelle, K. N. (2017). Hippocampal atrophy and altered brain responses to pleasant tastes among obese compared with healthy weight children. *International Journal of Obesity (2005)*, *41*(10), 1496–1502. https://doi.org/10.1038/ijo.2017.130

Myers, M., Britt, K. L., Wreford, N. G. M., Ebling, F. J. P., & Kerr, J. B. (2004). Methods for quantifying follicular numbers within the mouse ovary. *Reproduction (Cambridge, England)*, *127*(5), 569–580. https://doi.org/10.1530/rep.1.00095

Nantie, L. B., Himes, A. D., Getz, D. R., & Raetzman, L. T. (2014). Notch signaling in postnatal pituitary expansion: Proliferation, progenitors, and cell specification. *Molecular Endocrinology (Baltimore, Md.)*, *28*(5), 731–744. https://doi.org/10.1210/me.2013-1425

O'Toole, K. K., Hooper, A., Wakefield, S., & Maguire, J. (2014). Seizure-induced disinhibition of the HPA axis increases seizure susceptibility. *Epilepsy Research*, *108*(1), 29–43. https://doi.org/10.1016/j.eplepsyres.2013.10.013

Pantier, L. K., Li, J., & Christian, C. A. (2019). Estrous Cycle Monitoring in Mice with Rapid Data Visualization and Analysis. *Bio-Protocol*, *9*(17), e3354. https://doi.org/10.21769/BioProtoc.3354

Paxinos, G., & Keith B.J. Franklin. (2019). *The Mouse Brain in Stereotaxic Coordinates* (5th ed.). Academic Press.

Phuong, T. H., Houot, M., Méré, M., Denos, M., Samson, S., & Dupont, S. (2021). Cognitive impairment in temporal lobe epilepsy: Contributions of lesion, localization and lateralization. *Journal of Neurology*, *268*(4), 1443–1452. https://doi.org/10.1007/s00415-020-10307-6

Racine, R. J. (1972). Modification of seizure activity by electrical stimulation. II. Motor seizure. *Electroencephalography and Clinical Neurophysiology*, *32*(3), 281–294. https://doi.org/10.1016/0013-4694(72)90177-0

Rattka, M., Brandt, C., & Löscher, W. (2013). The intrahippocampal kainate model of temporal lobe epilepsy revisited: Epileptogenesis, behavioral and cognitive alterations, pharmacological response, and hippoccampal damage in epileptic rats. *Epilepsy Research*, *103*(2–3), 135–152. https://doi.org/10.1016/j.eplepsyres.2012.09.015

Riban, V., Bouilleret, V., Pham-Lê, B. T., Fritschy, J.-M., Marescaux, C., & Depaulis, A. (2002). Evolution of hippocampal epileptic activity during the development of hippocampal sclerosis in a mouse model of temporal lobe epilepsy. *Neuroscience*, *112*(1), 101–111. https://doi.org/10.1016/s0306-4522(02)00064-7

Scharfman, H. E., Kim, M., Hintz, T. M., & MacLusky, N. J. (2008). Seizures and reproductive function: Insights from female rats with epilepsy. *Annals of Neurology*, *64*(6), 687–697. https://doi.org/10.1002/ana.21518

Shinohara, Y., Hirase, H., Watanabe, M., Itakura, M., Takahashi, M., & Shigemoto, R. (2008). Left-right asymmetry of the hippocampal synapses with differential subunit allocation of glutamate receptors. *Proceedings of the National Academy of Sciences of the United States of America*, *105*(49), 19498–19503. https://doi.org/10.1073/pnas.0807461105

Shipton, O. A., El-Gaby, M., Apergis-Schoute, J., Deisseroth, K., Bannerman, D. M., Paulsen, O., & Kohl, M. M. (2014). Left–right dissociation of hippocampal memory processes in mice. *Proceedings of the National Academy of Sciences*, *111*(42), 15238–15243. https://doi.org/10.1073/pnas.1405648111

Sullivan, S. D., & Moenter, S. M. (2004). Prenatal androgens alter GABAergic drive to gonadotropin-releasing hormone neurons: Implications for a common fertility disorder. *Proceedings of the National Academy of Sciences of the United States of America*, *101*(18), 7129–7134. https://doi.org/10.1073/pnas.0308058101

Sutula, T., Cascino, G., Cavazos, J., Parada, I., & Ramirez, L. (1989). Mossy fiber synaptic reorganization in the epileptic human temporal lobe. *Annals of Neurology*, *26*(3), 321–330. https://doi.org/10.1002/ana.410260303

Tabibnia, G., Cooke, B. M., & Breedlove, S. M. (1999). Sex difference and laterality in the volume of mouse dentate gyrus granule cell layer. *Brain Research*, *827*(1–2), 41–45. https://doi.org/10.1016/s0006-8993(99)01262-7

Teede, H. J., Joham, A. E., Paul, E., Moran, L. J., Loxton, D., Jolley, D., & Lombard, C. (2013). Longitudinal weight gain in women identified with polycystic ovary syndrome: Results of an observational study in young women. *Obesity (Silver Spring, Md.)*, *21*(8), 1526–1532. https://doi.org/10.1002/oby.20213

Ueno, N., Ling, N., Ying, S. Y., Esch, F., Shimasaki, S., & Guillemin, R. (1987). Isolation and partial characterization of follistatin: A single-chain Mr 35,000 monomeric protein that inhibits the release of follicle-stimulating hormone. *Proceedings of the National Academy of Sciences of the United States of America*, *84*(23), 8282–8286. https://doi.org/10.1073/pnas.84.23.8282

Woodruff, T. K., & Mayo, K. E. (1990). Regulation of inhibin synthesis in the rat ovary. *Annual Review of Physiology*, *52*, 807–821. https://doi.org/10.1146/annurev.ph.52.030190.004111

Yasin, M., Dalkin, A. C., Haisenleder, D. J., Kerrigan, J. R., & Marshall, J. C. (1995). Gonadotropin-releasing hormone (GnRH) pulse pattern regulates GnRH receptor gene expression: Augmentation by estradiol. *Endocrinology*, *136*(4), 1559–1564. https://doi.org/10.1210/endo.136.4.7895666

Ying, S. Y. (1988). Inhibins, activins, and follistatins: Gonadal proteins modulating the secretion of follicle-stimulating hormone. *Endocrine Reviews*, *9*(2), 267–293. https://doi.org/10.1210/edrv-9-2-267

Tables:

Table 1. Primer sequences. List of the primer sequences for the gonadotropins (*Lhb, Fshb*), *Gnrhr,* and control *Ppia* used for qPCR.

Gene	Forward Sequence 5'-3'	Reverse sequence 3'-5'
Ppia	CAAATGCTGGACCAAACACAAACG	GTTCATGCCTTCTTTCACCTTCCC
Lhb	CCCAGTCTGCATCACCTTCAC	GAGGCACAGGAGGCAAAGC
Fshb	TGGTGTGCGGGCTACTGCTAC	ACAGCCAGGCAATCTTACGGTCTC
Gnrhr	ATGATGGTGGTGATTAGCC	ATTGCGAGAAGACTGTGG

Table 2. Statistical parameters for hippocampal sclerosis measures

	n	Results
I:C ratio (two-way ANOVA)		
Panel B	18 control left 18 control right 26 IHKA left 26 IHKA right	Control vs IHKA: $F(1, 85) = 13.82$, $p = 0.0004$ Left vs right: $F(1, 85) = 6.40$, $p = 0.01$ Interaction: $F(1,85) = 2.64$, $p = 0.11$
Proportion of mice with I:C ratio >1.5 (Chi-square test)		
Panel C	18 IHKA left no dispersion 8 IHKA left dispersion 12 IHKA right no dispersion 15 IHKA right dispersion	$\chi^2 = 2.49$, $df = 1$, $p = 0.11$

Table 3. Statistical parameters for estrous cycle measures

	n	Results
Cycle length (two-way ANOVA)		
One month	42 control left 59 control right 47 IHKA left 56 IHKA right	Control v IHKA: F(1, 209) = 9.23, p = 0.002 Left vs right: F(1, 209) =0.143 , p = 0.71 Interaction: F(1, 209) = 0.004 , p = 0.95
Two months	28 control left 45 control right 35 IHKA left 35 IHKA right	Control v IHKA: F(1,148) = 6.61, p = 0.01 Left vs right: F(1,148) = 0.49, p = 0.48 Interaction: F(1, 148) = 0.0097, p = 0.92
Four months	12 control left 19 control right 15 IHKA left 13 IHKA right	Control v IHKA: F(1,62) = 0.94, p = 0.33 Left vs right: F(1, 62) = 0.69, p = 0.41 Interaction: F(1, 62) = 1.87, p = 0.18
Proportions of mice with regular and long cycles (Chi-square test)		
Overall	62 IHKA L regular 44 IHKA L long 63 IHKA R regular 49 IHKA R long	χ^2= 0.039, df = 1, p =0.84
One month	29 IHKA left regular 21 IHKA left long 29 IHKA right regular 30 IHKA right long	χ^2= 0.53266, df = 1, p = 0.47
	29 control right regular 30 control right long 51 IHKA right regular 9 IHKA right long	χ^2=15.76, df = 1, p = 7.2 x 10^{-5}
	29 control left regular 21 control left long 36 IHKA left regular 8 IHKA left long	χ^2= 5.15, df = 1, p = 0.02
Two months	21 IHKA left regular 17 IHKA left long 25 IHKA right regular 13 IHKA right long	χ^2= 0.49565, df = 1, p = 0.48
	39 control right regular 7 control right long 25 IHKA right regular 13 IHKA right long	χ^2= 3.1574, df = 1, p = 0.076
	23 control left regular 7 control left long 21 IHKA left regular 17 IHKA left long	χ^2= 2.491, df = 1, p = 0.11
Four months	12 IHKA left regular 6 IHKA left long 9 IHKA right regular 6 IHKA right long	χ^2= 0.0010913, df = 1, p = 0.97

	19 control right regular 0 control right long 9 IHKA right regular 6 IHKA right long	χ^2=6.68, df = 1, p = 0.009
	12 control left regular 2 control left long 12 IHKA left regular 6 IHKA left long	χ^2= 0.67725, df = 1, p = 0.41

Table 4. Three-way ANOVA for hormone measures

	n	Results
Estradiol 28 control left 23 control right 31 IHKA left 29 IHKA right	Plate 1: 11 control left 9 control right 7 IHKA left 4 IHKA right Plate 2: 12 control left 4 control right 6 IHKA left 2 IHKA right Plate 3: 4 control left 2 control right 14 IHKA left 12 IHKA right Plate 4: 1 control left 8 control right 4 IHKA left 11 IHKA right	Control vs IHKA: $F(1,104) = 0.44$, $p = 0.50$ Left vs right: $F(1, 104) = 0.22$, $p = 0.63$ Plate: $F(3, 104) = 9.27$, $p = 1.74 \times 10^{-5}$ Treatment by side: $F(1, 104) = 3.18$, $p = 0.08$
Progesterone 26 control left 32 control right 32 IHKA left 30 IHKA right	Plate 1: 8 control left 7 control right 9 IHKA left 4 IHKA right Plate 2: 13 control left 9 control right 5 IHKA left 1 IHKA right Plate 3: 3 control left 3 control right 12 IHKA left 14 IHKA right Plate 4: 2 control left 13 control right 6 IHKA left 11 IHKA right	Control vs IHKA: $F(1,113) = 1.95$, $p = 0.17$ Left vs right: $F(1, 113) = 0.13$, $p = 0.71$ Plate: $F(3,113) = 2.27$, $p = 0.08$ Treatment by side: $F(1, 113) = 0.02$, $p = 0.89$
Testosterone	Plate 1: 10 control left	Control vs IHKA: $F(1,129) = 0.02$, $p = 0.88$ Left vs right: $F(1,129) = 0.45$, $p = 0.50$

37 control left 33 control right 32 IHKA left 34 IHKA right	7 control right 7 IHKA left 7 IHKA right <u>Plate 2:</u> 20 control left 10 control right 6 IHKA left 2 IHKA right <u>Plate 3:</u> 4 control left 3 control right 13 IHKA left 13 IHKA right <u>Plate 4:</u> 3 control left 13 control right 6 IHKA left 12 IHKA right	Plate: $F(3, 129)= 6.97$, $p= 0.0002$ Treatment by side: $F(1,129) =1.15$, $p = 0.29$
Corticosterone 5 control left 27 control right 14IHKA left 23 IHKA right	<u>Plate 1:</u> 3 control left 13 control right 8 IHKA left 13 IHKA right <u>Plate 2:</u> 2 control left 14 control right 6 IHKA left 10 IHKA right	Control vs IHKA: $F(1,64) = 1.55$, $p = 0.22$ Left vs right: $F(1,64) = 0.025$, $p = 0.87$ Plate: $F(1,64) =1.29$, $p = 0.26$ Treatment by side: $F(1,64) =0.99$, $p = 0.32$

Table 5. **Ovarian follicle counts are unchanged with differing site of injection and independent of injection type.** Means ± SEM of primary, secondary, and antral follicles as well as corpora lutea for each treatment group. Comparisons between injection type (Con or IHKA), and injection laterality (left or right) were made by two-way ANOVA.

	Control		**IHKA**		**F-Value**	**P-Value**
Follicle Type	Left	Right	Left	Right		
Primary	1.66 ± 1 .02	1.55 ± 1.17	1.51 ± 0.98	1.60 ± 1.07	0.22	0.88
Secondary	3.11 ± 1.80	2.80 ± 1.90	2.90 ± 1.73	3.21 ± 1.56	0.53	0.66
Antral	3.32 ± 1.27	3.49 ± 1.33	3.56 ± 1.47	3.57 ± 1.46	0.33	0.81
Corpora Lutea	2.27 ± 1.01	2.07 ± 1.07	1.84 ± 1.06	1.98 ± 1.06	1.34	0.26

Table 6. Two-way ANOVA for pituitary mRNA expression measures

	n	Results
Fshb	11 control left 13 control right 8 IHKA left 13 IHKA right	Control vs IHKA: $F(1, 41) = 0.02$, $p = 0.89$ Left vs right: $F(1, 41) = 6.87$, $p = 0.01$ Treatment by side: $F(1, 41) = 5.88$, $p = 0.02$
Lhb	11 control left 13 control right 8 IHKA left 13 IHKA right	Control vs IHKA: $F(1,41) = 4.35$, $p = 0.04$ Left vs right: $F(1, 41) = 10.19$, $p = 0.003$ Treatment by side: $F(1, 41) = 2.03$, $p = 0.16$
Gnrhr	14 control left 13 control right 16 IHKA left 13 IHKA right	Control vs IHKA: $F(1, 52) = 4.53$, $p = 0.04$ Left vs right: $F(1, 52) = 5.61$, $p = 0.02$ Treatment by side: $F(1, 52) = 0.40$, $p = 0.53$

Table 7. Three-way ANOVA for weight gain measures

	n	Results
One month	14 control left 8 control right 10 IHKA left 8 IHKA right	Control vs IHKA: $F(1,162) = 19.25$, $p = 2.06 \times 10^{-5}$ Left vs right: $F(1,162) = 5.56$, $p = 0.02$ Month: $F(2,162) = 4.09$, $p = 0.019$ Treatment by side: $F(1,162) = 0.71$, $p = 0.40$ Treatment by month: $F(1, 162) = 3.82$, $p = 0.02$ Side by month: $F(1, 162) = 2.04$, $p = 0.13$ Treatment by month by side: $F(1, 162) = 0.80$, $p = 0.45$
Two months	19 control left 28 control right 18 IHKA left 14 IHKA right	
Four months	10 control left 15 control right 15 IHKA left 15 IHKA right	

Figure Legends:

Figure 1. Experimental timeline. Schematic of procedures and timepoints for each component. Note that each timepoint category has 4 groups: IHKA-L, IHKA-R, Con-L, and Con-R. At the time of euthanasia, trunk blood, pituitary, brain, and ovaries were collected from each animal. wpi = weeks post-injection.

Figure 2. Outcomes for seizure screening and histology for confirmation of IHKA injection. (A) Numbers of mice that did and did not show at least one seizure on video collected 3-5 hours after intrahippocampal injection. (B) Inclusion numbers and criteria based on Nissl and GFAP staining for mice that did not show seizures immediately following injection. (C) Inclusion numbers and criteria based on Nissl and GFAP staining for mice that did show seizures immediately following injection. (D) Total number of animals included in each group within the sclerosis data set.

Figure 3. Higher degree of hippocampal sclerosis in IHKA-R compared with IHKA-L mice. **(**A) Representative images of Nissl (left) and GFAP staining (right). (B) Individual ipsilateral:contralateral ratio of each mouse with mean ± SEM for each treatment group. * $p < 0.05$, *** $p < 0.001$ for comparisons between injection type (Con or IHKA), and injection side (left or right) by two-way ANOVA and Tukey's post hoc test. (C) Percentages of mice that developed an I:C ratio of granule cell dispersion >1.5 (dark gray bars) and those that did not (light gray bars).

Figure 4. Estrous cycle period is lengthened after IHKA injection. (A) Representative examples of a regular estrous cycle seen in a saline-injected control (left), an IHKA mouse with

a regular 4-6 d cycle (middle), and an IHKA mouse with a long (≥7 day) cycle (right). (B) Cycle length of each mouse in the study at each post-injection timepoint with mean ± SEM. * $p < 0.05$, ** $p < 0.01$ for comparisons between injection type (Con or IHKA), and injection side (left or right) and month timepoint (one, two, or four) by three-way ANOVA and Tukey's post hoc test. (C) Percentages of mice that developed long cycles (dark gray bars) and those that retained a regular cycle (light gray bars). Comparisons made by chi-squared tests.

Figure 5. **Ovarian hormones do not change with IHKA injection or laterality.** Individual estradiol (top), progesterone (middle), and testosterone (bottom) values for each mouse with mean ± SEM for each treatment. Comparisons between injection type (Con or IHKA), and injection side (left or right) and ELISA plate made by three-way ANOVA.

Figure 6. Lateralized differences in pituitary *Fshb, Lhb,* and *Gnrhr* gene expression two months after injection. Individual mean fold change values for each control and IHKA mouse for *Fshb* (A), *Lhb* (B), and *Gnrhr* (C), with mean ± SEM for each treatment group. * $p \leq 0.05$, ** $p < 0.01$ for comparisons between injection type (Con or IHKA), and injection side (left or right) by two-way ANOVA and Tukey's post hoc test.

Figure 7. Post-injection weight gain of mice euthanized at one, two, or four months. Individual weight gain values derived from differences in values measured at the time of injection to the time of tissue collection for each Con and IHKA mouse, with mean ± SEM for each treatment group. * $p < 0.05$, ** $p < 0.01$ for comparisons between injection type (Con or IHKA), and injection laterality (left or right), and post-injection time (one, two, or four months) by three-way ANOVA and Tukey's post hoc test.

Figure 8. Summary of results. Outcomes of IHKA injections into the left or right dorsal hippocampus.

Figure 1

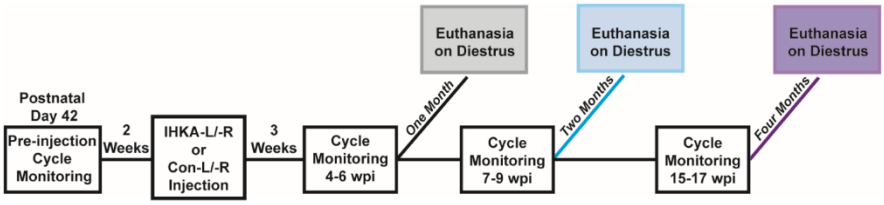
Postnatal Day 42
Pre-injection Cycle Monitoring
2 Weeks
IHKA-L/-R or Con-L/-R Injection
3 Weeks
Cycle Monitoring 4-6 wpi
One Month
Euthanasia on Diestrus
Cycle Monitoring 7-9 wpi
Two Months
Euthanasia on Diestrus
Cycle Monitoring 15-17 wpi
Four Months
Euthanasia on Diestrus

Figure 2

A

	Video Screening for Acute Seizures	
	≥ 1 seizure	*No seizures on video*
IHKA-L	21	12
IHKA-R	18	12

B

	Histology for mice without seizures on video			
	Sclerosis	*Gliosis*	*No sclerosis or gliosis*	Included
IHKA-L	5	3	4	8
IHKA-R	9	1	2	10

C

	Histology for mice with seizures on video			
	Sclerosis	*Gliosis*	*No sclerosis or gliosis*	Included
IHKA-L	14	4	3	18
IHKA-R	13	3	2	16

D

	Mice included in the sclerosis data set
IHKA-L	26
IHKA-R	26

Figure 3

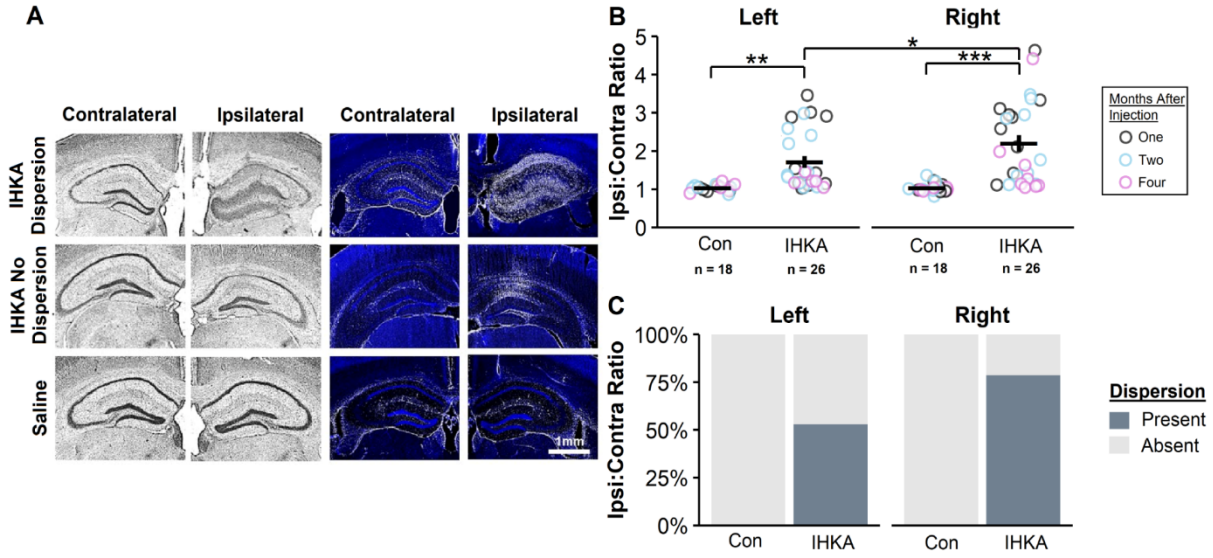
A
Contralateral
Ipsilateral
Contralateral
Ipsilateral
IHKA Dispersion
IHKA No Dispersion
Saline
1mm
B
Left
Right
Ipsi:Contra Ratio
**
*
***
Con
IHKA
Con
IHKA
n = 18
n = 26
n = 18
n = 26
Months After Injection
One
Two
Four
C
Left
Right
Ipsi:Contra Ratio
100%
75%
50%
25%
0%
Con
IHKA
Con
IHKA
Dispersion
Present
Absent

Figure 4

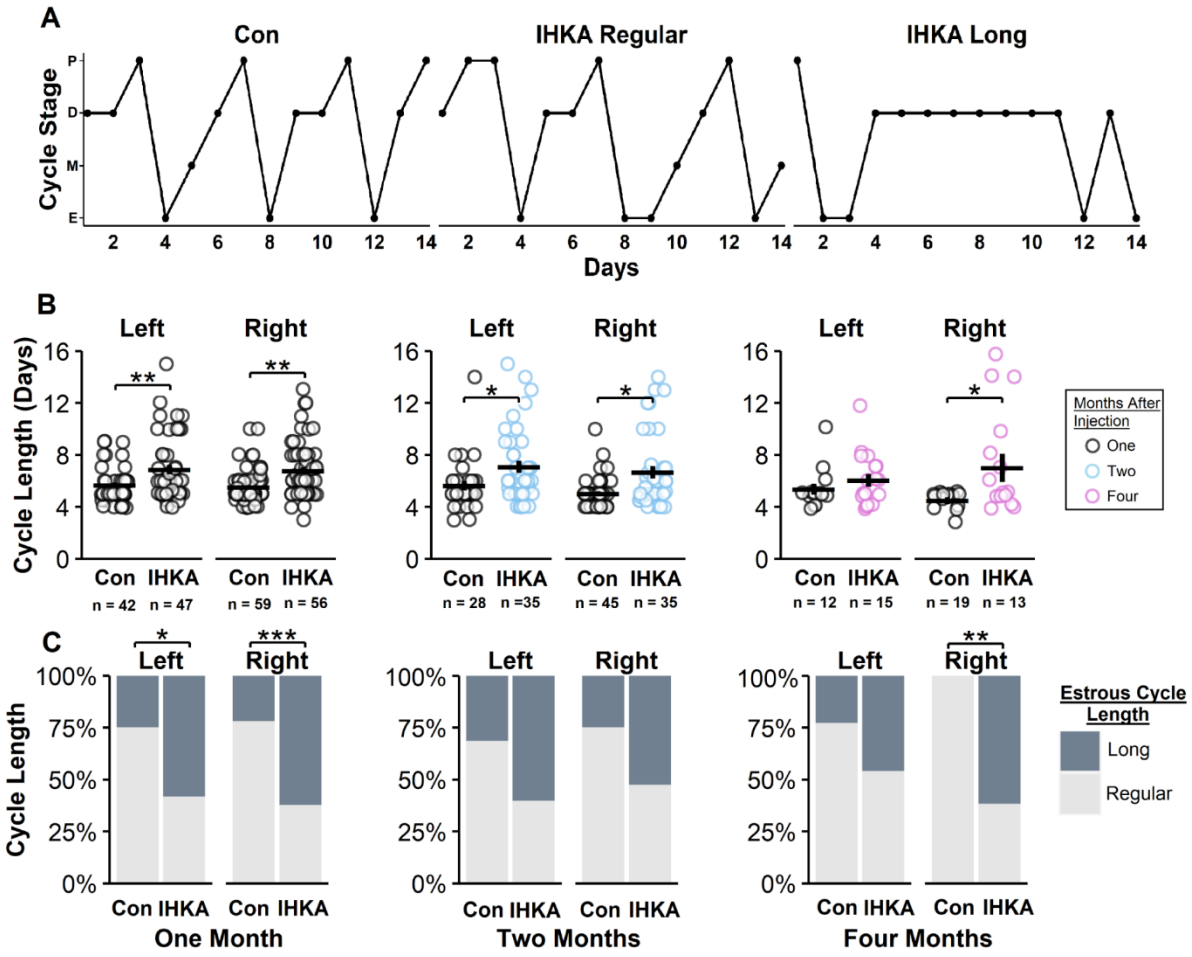
A
Con
IHKA Regular
IHKA Long
Cycle Stage
P
D
M
E
2 4 6 8 10 12 14
Days
B
Left
Right
Cycle Length (Days)
Con IHKA
n = 42 n = 47
n = 59 n = 56
n = 28 n =35
n = 45 n = 35
n = 12 n = 15
n = 19 n = 13
Months After Injection
One
Two
Four
C
Cycle Length
100%
75%
50%
25%
0%
Con IHKA
One Month
Two Months
Four Months
Estrous Cycle Length
Long
Regular

Figure 5

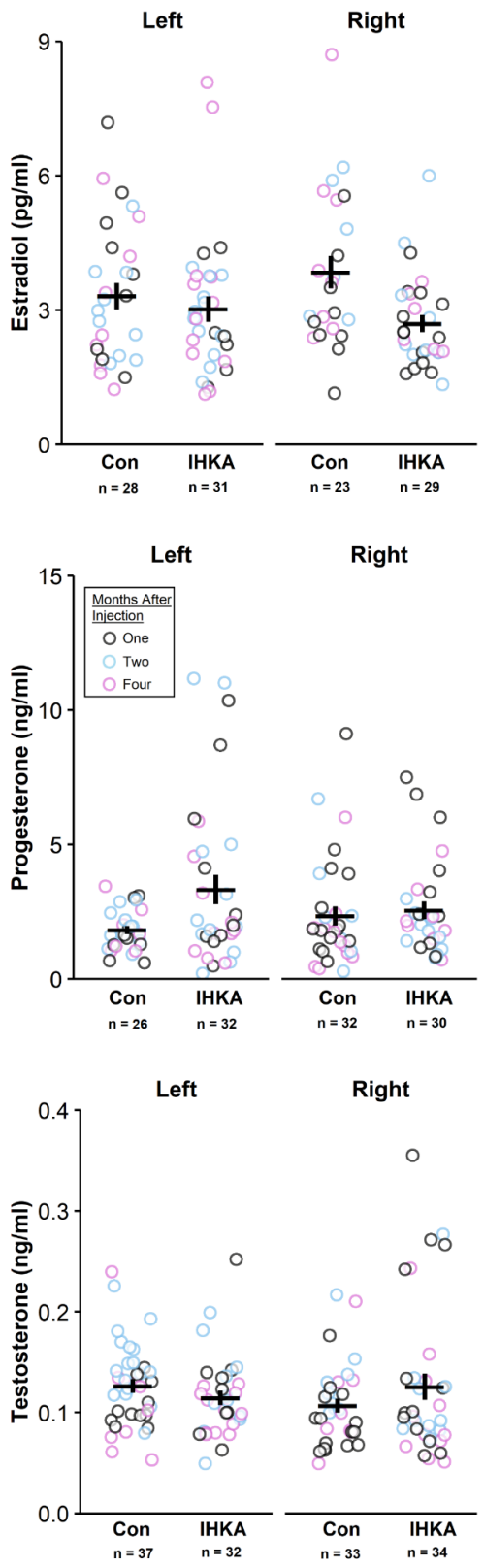
Left
Right
Estradiol (pg/ml)
9
6
3
0
Con
n = 28
IHKA
n = 31
Con
n = 23
IHKA
n = 29
Left
Right
Progesterone (ng/ml)
15
10
5
0
Months After Injection
One
Two
Four
Con
n = 26
IHKA
n = 32
Con
n = 32
IHKA
n = 30
Left
Right
Testosterone (ng/ml)
0.4
0.3
0.2
0.1
0.0
Con
n = 37
IHKA
n = 32
Con
n = 33
IHKA
n = 34

Figure 6

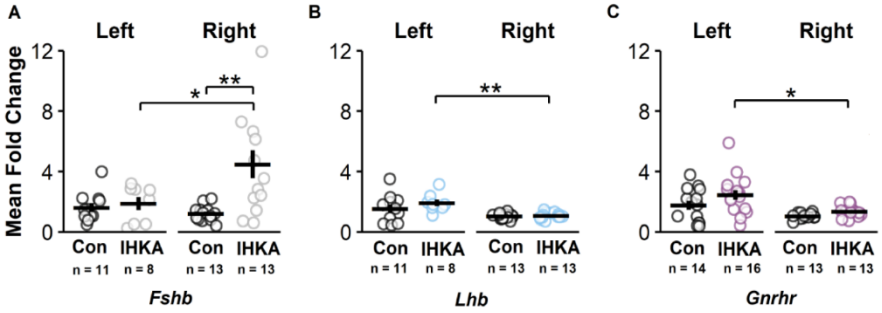
A
Left
Right
Mean Fold Change
12
8
4
0
*
**
Con
IHKA
Con
IHKA
n = 11
n = 8
n = 13
n = 13
Fshb
B
Left
Right
12
8
4
0
**
Con
IHKA
Con
IHKA
n = 11
n = 8
n = 13
n = 13
Lhb
C
Left
Right
12
8
4
0
*
Con
IHKA
Con
IHKA
n = 14
n = 16
n = 13
n = 13
Gnrhr

Figure 7

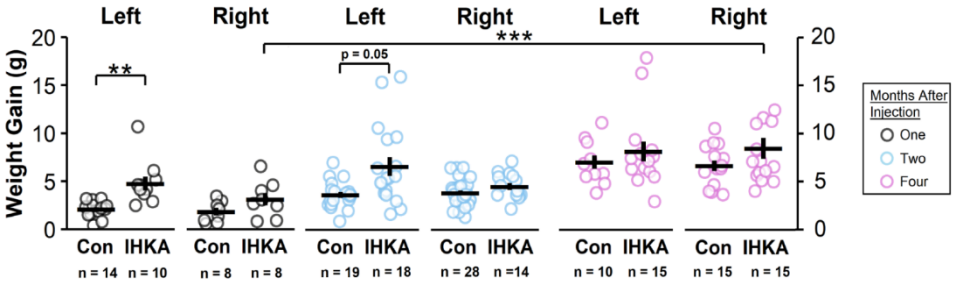
Left
Right
Left
Right
Left
Right
Weight Gain (g)
20
15
10
5
0
**
p = 0.05
***
Con
IHKA
n = 14
n = 10
n = 8
n = 8
n = 19
n = 18
n = 28
n =14
n = 10
n = 15
n = 15
n = 15
Months After Injection
One
Two
Four

Figure 8

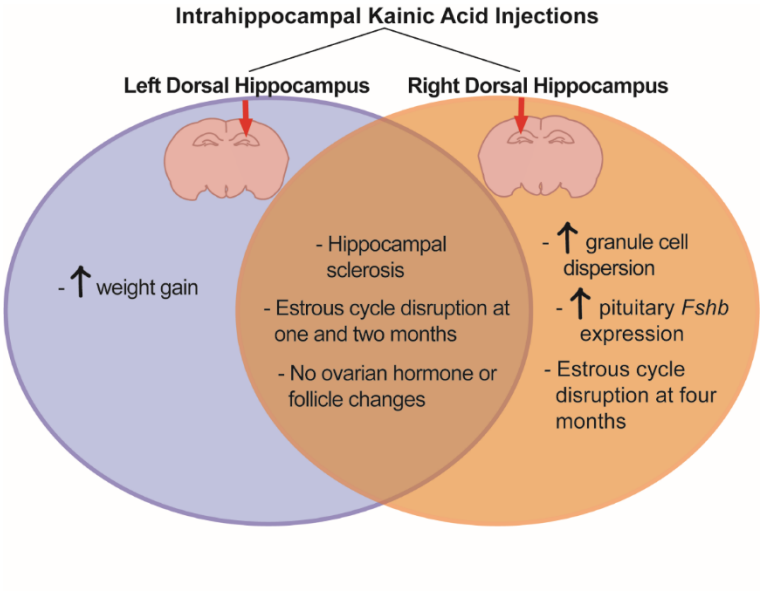
Intrahippocampal Kainic Acid Injections
Left Dorsal Hippocampus
Right Dorsal Hippocampus
- ↑ weight gain
- Hippocampal sclerosis
- Estrous cycle disruption at one and two months
- No ovarian hormone or follicle changes
- ↑ granule cell dispersion
- ↑ pituitary *Fshb* expression
- Estrous cycle disruption at four months